Antiferromagnetic Spin Structure and Domains in Exchange-Coupled Multilayers

C. L. Chien, V. S. Gornakov, V. I. Nikitenko, A. J. Shapiro, and R. D. Shull

***Abstract*—As revealed by the observation of memory effects and domain imaging, the antiferromagnetic (AFM) spin structure in exchange bias is not static. During reversal, the AFM spins form an exchange spring connected with the ferromagnet (FM). We have observed hybrid domain walls consisting of FM and AFM sections and their evolution using the magnetooptical indicator film technique. The external magnetic field moves only the FM section of the hybrid domain walls, leading to the formation of an exchange spring parallel to the interface. The nucleation and unwinding of the exchange spring occur at different locations, and the propagation depends strongly on the chirality of the FM domain walls.**

***Index Terms*—Antiferromagnetic (AFM), domain, exchange bias, spin structure.**

I. Introduction

EXCHANGE bias plays an essential role in spin-valve giant magnetoresistance (GMR) field sensors, which have already been employed in read-heads in hard drives [1], as well as in prototype nonvolatile memories based on magnetic tunnel junctions. However, despite the technical importance and intense interest in recent years [2]–[4], [21] in exchange bias, not to mention its discovery more than 40 years ago [5], [22], the understanding of many of its key aspects remains unsatisfactory.

The simplest geometry for observing and exploring exchange bias consists of a bilayer of a ferromagnet (FM) and antiferromagnet (AFM). After field-cooling, most commonly in a constant magnetic field, the hysteresis loop of the FM becomes shifted away from the origin by the amount known as the exchange field H_E, accompanied by an enhanced coercivity H_c. The shifted hysteresis loop, with a unidirectional anisotropy, no longer exhibits the usual symmetry of $M(H) = -M(-H)$ of a single FM layer. In this respect, the underlying AFM layer serves the purpose of "pinning" the adjacent FM layer, a feature exploited in the spin-valve GMR sensors.

Since the discovery of exchange bias, it has been recognized that the AFM spin structure is central to understanding the phenomenon. To account for the shifted FM loop, the AFM surface spin structure would necessarily have an uncompensated magnetization at the FM/AFM interface due to the spin structure of the AFM layer and/or due to extrinsic causes such as interface roughness. Furthermore, the AFM layer must have a sufficiently large AFM anisotropy to withstand the reversal of the FM layer. These aspects have been incorporated in most theoretical models.

Various theoretical models that have been proposed to account for exchange bias differ in the AFM spin structure. The earliest model and some of the current models have assumed a static AFM spin structure [5], [22]. The exchange bias is entirely due to the interactions among the FM and the uncompensated AFM moments at or near the FM/AFM interface. After field-cooling, the AFM spin structure, henceforth, remains fixed even during the magnetization reversal of the FM layer. Aside from discrepancies in the predicted values of H_E and H_c, a number of key predictions of the static models are contrary to experiments. Since the static models are based on interfacial interactions with a fixed AFM spin structure, the thickness of the AFM layer would not be of consequence. Experimentally, the values of H_E and H_c have been found to depend strongly on an AFM layer thickness of as much as 500 Å [6]. With a static AFM spin structure, the characteristics of forward magnetization switching (from H to $+H$) and the reversed switching (from $+H$ to $-H$) parts of the FM layer would be symmetrical. Yet, the observed switching events have been found to be distinctly asymmetrical [7], [8]. The memory effects [9], [10], which will be discussed briefly in the following, are also in variance with the predictions of the static models.

Several theoretical models of exchange bias, from either energy consideration or more detailed micromagnetic calculations, have concluded that AFM spin structure cannot be static [11]–[15], [23]. In the ground state, the AFM and the FM spin structures are coupled due to the strong interactions at the interface. However, the AFM spin structure changes during the magnetization reversal of the FM layer. Specifically, when the magnetization of the FM is reversed, the AFM moments fan out into a spiraling spin structure, or an exchange spring, which connects the FM layer at the FM/AFM interface and extends well within the AFM layer. This spiraling spin structure was first concluded in [11] and subsequently by several other theoretical studies [12]–[15], [23]. Evidence of a spiraling AFM spin structure has recently been indicated in special FM1/AFM/FM2 trilayers with an AFM spin structure coupled between two FM layers of opposite magnetizations [16].

Manuscript received February 15, 2002; revised May 13, 2002. The work at JHU was supported by the National Science Foundation under Grant DMR00-80031 and Grant DMR01-01814.

C. L. Chien is with the Department of Physics and Astronomy, The Johns Hopkins University, Baltimore, MD 21218 USA.

V. S. Gornakov is with the National Institute of Standards and Technology, Gaithersburg, MD 20899 USA and also with the Institute of Solid State Physics, Russian Academy of Sciences, Chernogolovka 142432, Russia.

V. I. Nikitenko is with the Department of Physics and Astronomy, The Johns Hopkins University, Baltimore, MD 21218 USA, the National Institute of Standards and Technology, Gaithersburg, MD 20899 USA, and also with the Institute of Solid State Physics, Russian Academy of Sciences, Chernogolovka 142432, Russia.

A. J. Shapiro and R. D. Shull are with the National Institute of Standards and Technology, Gaithersburg, MD 20899 USA.

Digital Object Identifier 10.1109/TMAG.2002.803169.

The importance of spiraling in exchange bias notwithstanding, thin AFM layers in general and its AFM spin structure in particular are not easily accessible to direct experimental studies. Furthermore, recent work [17] shows that the surface AFM spin structure is dramatically altered after the FM layer has been deposited on the AFM layer. Thus, an isolated AFM is unlikely to provide useful information about exchange bias, which must be gained from the studies of FM/AFM multilayers. Magnetic imaging techniques, more specifically under an external magnetic field, will be crucial in revealing the microscopic switching events. In this respect, the imaging techniques that utilize an electron beam would not be amenable to an external field, whereas an optical imaging technique would be.

In this work, we describe several experiments in which we utilized the FM layers in suitably structured bilayers to provide information of the underlying AFM layer. Using a optical domain imaging technique with an external magnetic field, we obtained information concerning the AFM spin structure, the AFM domains, the ground state spin structure near the FM/AFM interface, and the nucleation and motion of the domain wall in the exchange-coupled FM layer.

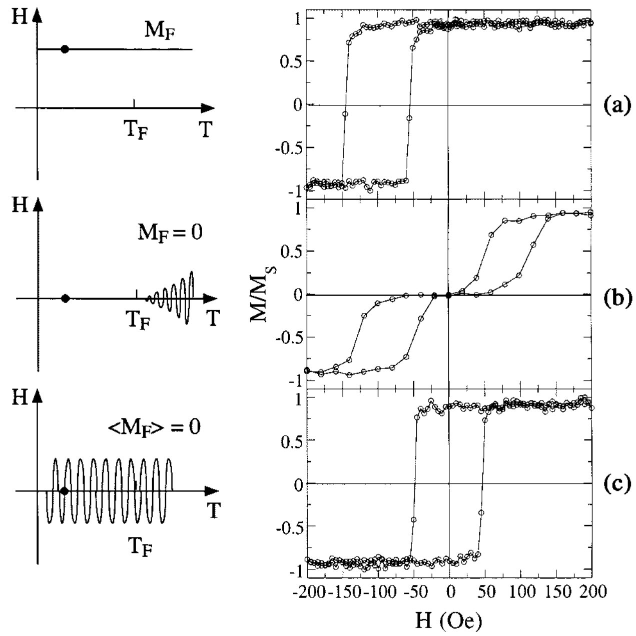

Fig. 1. Hysteresis loops of Py–CoO at 200 K. (a) After being field-cooled in a 200-Oe field. (b) After being demagnetized at 300 K and then cooled in zero field. (c) Cooled in an ac 200-Oe field at 1/4 Hz. The cooling procedures are schematically shown on the left.

II. Experiment

We have used two common FM/AFM bilayer systems of Py(175 Å)/CoO(370 Å) and Py(160 Å)/FeMn(300 Å) with the same FM $=$ Py $=$ $Ni_{81}Fe_{19}$, one with an insulating AFM $=$ CoO and the other a metallic AFM $=$ FeMn. We have used a vibrating sample magnetometer to measure the hysteresis loops, which give macroscopic information of switching. The magnetooptical indicator film (MOIF) technique has been used to observe the magnetic domains and reversal processes microscopically at the FM surface. As described elsewhere, the MOIF technique measures the stray magnetic field in the sample due to magnetization at the FM domain walls, defects in the sample, and at the sample edge [18]. In the domain pattern shown in Fig. 4, an arrow directed from the "black" edge toward the "white" edge indicates the magnetization direction in a domain. The key advantage of the MOIF technique is the application of an external magnetic field during measurements.

III. Memory Effects of Exchange Bias

In setting exchange bias, it is critically important to specify the conditions for the field-cooling process. Here we discuss the case of Py–CoO. Given the value of the Néel temperature of $T_N = 292$ K of CoO, we began the field-cooling process from 300 K. To illustrate different effects, the same Py–CoO bilayer has been subjected to several different field-cooling processes:

a) FC: Field-cooled (FC) the sample in a constant field of 200 Oe from $T > T_N$ to lower temperatures as schematically shown in the lef side of Fig. 1(a).
b) DM + ZFC: Demagnetize (DM) the FM layer with $M = 0$ by an ac field of decreasing magnitude at $T > T_N$, and then zero-field-cooled (ZFC) to lower temperatures as schematically shown in the left side of Fig. 1(b).
c) ACFC: Field cool (FC) the sample in an ac magnetic field of 200 Oe at 1/4 Hz with time-varying $\langle M \rangle$ averaged to 0, as schematically shown on the left of Fig. 1(c).
d) ACFC + FC: ACFC the sample to T_s followed by FC from T_s to lower temperatures, i.e., combining procedures c) and a).
e) FC + RFC: FC the sample to T_q, at which the direction of the magnetic field is reversed and FC to lower temperatures.

The resultant hysteresis loops measured at 200 K after procedures a)–c) are shown in Fig. 1(a)–(c), respectively. Procedure a) is the normal field-cooling procedure with the FM magnetization maintained at $M = M_s$, the saturation magnetization. This procedure results in a shifted hysteresis loop shown in Fig. 1(a). Using procedure b), field-cooling with zero magnetization of the FM layer ($M = 0$) results in two loops, shifted to both sides of $H = 0$ as shown in Fig. 1(b). Using procedure c), the time-averaged magnetization of the FM layer $\langle M \rangle = 0$ during field-cooling, with which one obtains an unshifted loop, as shown in Fig. 1(c). These very different results, measured from the same bilayer at the same temperature (200 K), illustrate vividly two important aspects of field-cooling that establish the exchange bias: the magnetization state of the FM layer and the entire history of cooling.

To further illustrate the second aspect, we can combine two procedures during the field-cooling process. When procedure a) is used, the resultant H_E value decreases with increasing temperature and vanishes at $T_N = 292$ K as shown in Fig. 2(a) labeled as "FC." Whereas, using procedure c), one observes no H_E for the entire temperature range, shown in Fig. 2(a) labeled as "ACFC." However, in procedure d), we have used ACFC to 260 K and then C from $T_s = 260$ K to 200 K. Successive measurements from 200 K to 300 K show that the H_E value de-

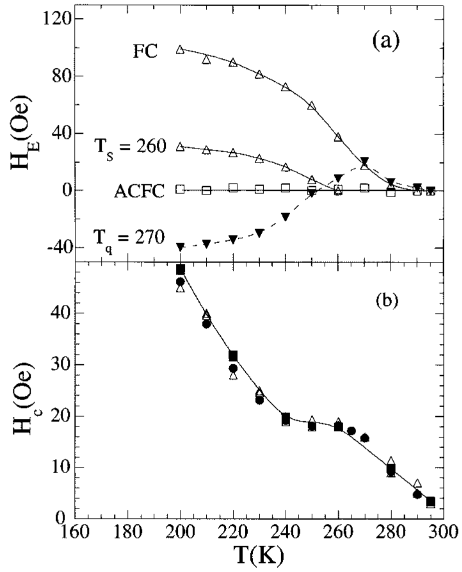

Fig. 2. Temperature dependence of (a) H_E of Py–CoO for field cool (FC), demagnetized and field cooled at $T_s = 260$ K, field cool to $T_q = 270$ K and reverse the field, and ac field cooled (ACFC) and (b) H_c of Py–CoO.

creases and vanishes at 260 K and remains so at higher temperatures, as shown in Fig. 2(a) labeled as "$T_s = 260$." Evidently, the bilayer "remembers" that field-cooling commenced at $T_s = 260$ K. As an another example, in procedure e), where we FC the sample to 270 K, at which we have reversed the magnetic field from $T_q = 270$–200 K. Successive measurements from 200 K to 300 K show that the H_E value is now negative at low temperatures. The value of H_E increases and becomes positive at about 250 K. Finally, the H_E value decreases from $T_q = 270$ K until T_N, as shown in Fig. 2(a) labeled "$T_q = 270$." In this example, the bilayer "remembers" that the cooling field direction has been reversed at $T_q = 270$ K. All of these results illustrate the memory effects of exchange bias, indicating that the AFM spin structure changes for different field-cooling conditions.

Another important aspect is the values of H_E and H_c. As shown in Fig. 2(b), the standard FC in a constant field gives rise to the largest H_E value $H_E(\max)$ at each temperature. By using various different field-cooling procedures, because of the memory effects, one can acquire any value of H_E of either sign between $H_E(\max)$ and $+H_E$(max). However, regardless of the latitude in the values of H_E, the values of the coercivity H_c are independent of the field-cooling procedure and history. The value of H_c is unique at each temperature and monotonically decreasing with temperature and reaching the free layer value at T_N as shown in Fig. 2(b).

IV. Domain Imaging in Py–FeMn Bilayers

We next describe the domain observation using MOIF of Py(160-Å)/FeMn(300-Å) bilayers. Because of the higher T_N of the FeMn layer, field-cooling commenced at 400 K, and imaging took place at 300 K. After the bilayer has been field-cooled in a constant field, i.e., procedure a), one obtains a shifted loop at 300 K as shown in Fig. 3(a). After the bilayer has been ac demagnetized and cooled in a zero field, i.e.,

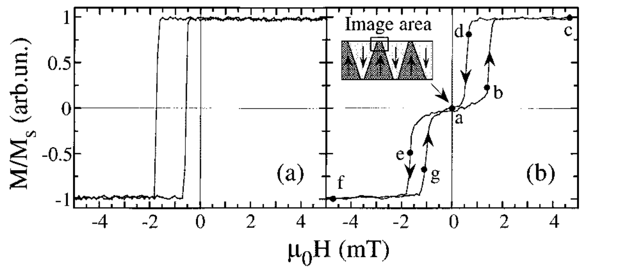

Fig. 3. Hysteresis loop of $Ni_{81}Fe_{19}$(160 Å)/FeMn(300 Å) at 300 K after (a) cooled in 1 T field from 400–300 K, and (b) ac demagnetized at 400 K and cooled in zero field to 300 K. Points (a), (b), (c), etc. correspond to the domain patterns in Fig. 4. The domain pattern and the image area are shown in the inset.

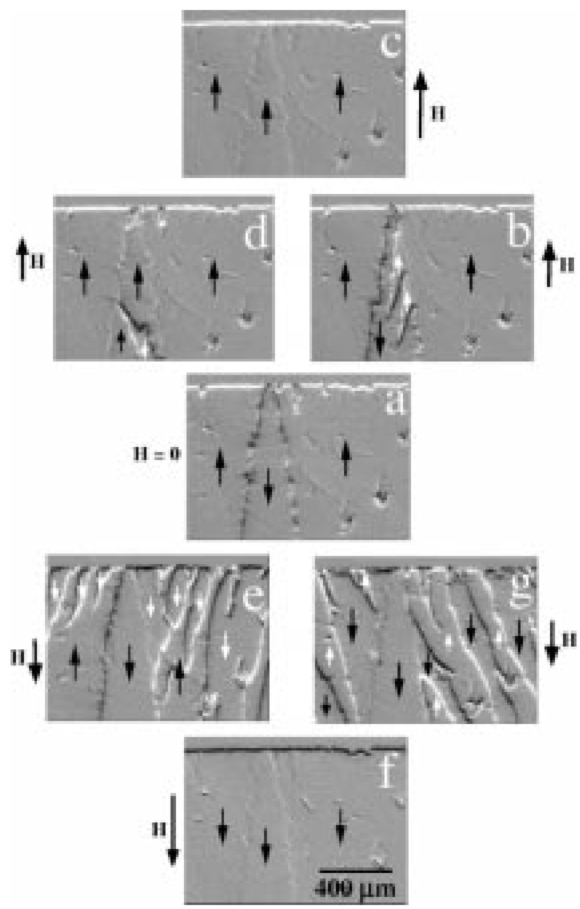

Fig. 4. MOIF image of domain patterns taken at various points (a, b, c, etc.) on the double hysteresis loop of Fig. 3(b) with the magnetic field $\mu_0 H$ of (a) 0, (b) 1.8, (c) 6, (d) 0.6, (e) -1.2 (f) -6, and (g) -0.35 mT. The black arrows indicate the magnetization direction of the domains, whereas the white arrows indicate those of the invading domains.

procedure c), one obtains two loops as shown in Fig. 3(b). The two loops in Fig. 3(b) are due to the ac demagnetization, which creates stripe domains with opposite magnetization. During the field-cooling in a zero field, half of the domains with one magnetization orientation acquire a positive bias field, while the other domains acquire a negative bias field. These stripe domains of opposite magnetization provide a favorable medium for observing the details of switching.

The MOIF microscope was focused on the DM+ZFC sample over one area about 1×1.5 mm near the sample edge, revealing three domains shown in Fig. 4(a), just as schematically shown in the insert of Fig. 3(b). We have arranged that the MOIF images in Fig. 4 correspond to various points on the double loop shown in Fig. 3(b), such that a, b, c, … in Fig. 4 correspond to points a, b, c, …, respectively labeled in Fig. 3(b).

Starting from the demagnetized state of point Fig. 4(a), the patterns (a)–(d) correspond to the right loop in Fig. 3(b) in the order of (a) ⇒ (b) ⇒ (c) ⇒ (d) ⇒ (a). From (a) ⇒ (b) ⇒ (c), the central "down" domain reverses to "up." This occurs with the invading domains (shown as white arrows) consuming the "down" regions in (b). Returning from (c) to (a) via (d), the invading "down" domains reverse the central "up" domain. Similarly, the patterns (a), (e), (f), and (g) in Fig. 4, corresponding to the negative loop in Fig. 3(b), show the domain reversal occurring in the two outer domains.

The domain patterns in Fig. 4 reveal several key aspects of exchange bias. In both (c) and (f), the F_M is in the single-domain state. However, the domain patterns of (d) and (e) [likewise by comparing (b) and (g)] are totally different, indicating an asymmetry in the nucleation of the domains for forward and backward reversal [7]. Furthermore, during reversal, only one of the two domain walls (DWs) shifts in order to accommodate the invading domains. This is clearly shown in (b) and (d) [and also in (e) and (f)] in which the invading domains nucleate and propagate at different locations. MOIF studies of the reversal processes of exchange-coupled FM/AFM bilayers uncover yet another unusual phenomena. One observes by comparing (b) with (d) for the central domain (likewise in (e) with (g) for the outer domains) that the invading domains are not along the easy axis, but are slanted in one direction during forward reversal and slanted in another direction for backward reversal. All of the acute asymmetry in both the nucleation domain and wall propagation in the magnetization reversal domain are key aspects of exchange-coupled FM/AFM bilayers due to an AFM spin structure that is not static.

Of particular interest are the AFM domains in thin AFM films exchange-coupled to FM. In uniform free FM layers, regardless of domain pattern, there are only mobile FM DWs, which can be swept by an external magnetic field into a single-domain state. The situation is very different in exchange-coupled FM/AFM bilayers. It is particularly revealing to compare (a), (c), and (f) in Fig. 4. In (a), two FM DWs separate three FM domains with opposite magnetizations, whereas in (c) and in (f) there is a single FM domain, which is unequivocally identified by the white edge in (c) and black edge in (f). Most remarkably, even in the single-domain FM of (c) and (f), there are still weaker but clearly visible contrasts at the original locations of the FM DW. These are the stationary AFM domain walls, which are not shifted by the applied field, thus revealing the underlying AFM domains. The weaker contrast of the AFM DW is due to FM spin frustration near its intersection with the FM/AFM interface. In this regard, the FM layer plays the role of a sensitive sensor through which stray fields at the AFM DW can be detected. It should be emphasized that when stripe domains have been created in a free FM layer, there will be no remnant traces of the original domain walls after the FM layer has been swept into the single-domain state by the external field. Only in an FM layer coupled with an AFM layer, such as that shown in (c) and (f) of Fig. 4, can one detect the contrast at the original locations of the FM DW when the FM layer has been swept into a single domain. These locations must be those of the AFM DW, which remain stationary.

In polycrystalline AFM thin films, the grain usually defines its own anisotropy axis. However, in FM/AFM bilayers, the FM sets the anisotropy axis of all the AFM grains that are in contact with a FM domain during field-cooling. The size of the AFM domain will be set by that of the FM domain. The results shown in Fig. 4(c) and (f) indeed reveal that the AFM domains have the same size as that of the FM domains, and remarkably, both are macroscopic in size on the submillimeter scale, four orders of magnitude larger than the AFM grain sizes. Thus, the observed results are not due to the altering of the orientations of the AFM grains during reversal as suggested by some studies, e.g., [19].

The above results clearly demonstrate the following important characteristics of exchange bias. First of all, the AFM spin structure is not static, or none of the asymmetry would be observed. Second, the spiraling AFM spin structure, or the exchange spring, is vertically connected with the FM magnetization. Third, the AFM spin structure has a chirality associated with it, as demonstrated by the invading domains that are slanted in one direction during forward reversal and slanted in another direction during the backward reversal. Fourth, the AFM domain walls in the lateral directions, established during the field-cooling process, remain stationary throughout the reversal of the FM layer. The emergent picture is that the AFM spin structure, established during field-cooling, becomes connected with the FM magnetization at the interface. When the FM magnetization is reversed, a spiral, or exchange spring, is formed within the underlying AFM spin structure from the interface penetrating into the interior of the AFM. Theoretical studies have indicated that the exchange spring has a depth δ of the order of $(A/K)^{1/2}$, where A and K are the exchange stiffness and anisotropy constant, respectively, of the AFM [11].

In Fig. 5(a), we schematically illustrate the situation of the ground state of the sample with stripe domains. There is a hybrid domain wall (HDW) consisting of both the FM DW (shaded region) and the AFM DW (hatched region). The external magnetic field moves only the FM DW but not the AFM DW. When the FM magnetization rotates in response to a magnetic field, the FM DW moves, as shown in Fig. 5(b), and the AFM spins near the interface are twisted into an exchange spring. This results in a new section of HDW that is parallel to the interface, advancing with the FM DW at one end and pinned at the AFM DW at the other end. In contrast to DW that moves readily in free FM films, in exchange-coupled FM/AFM bilayers, however, the moving FM DW carries with it the advancing exchange spring. This process impedes FM DW motion during the winding of the exchange spring. When the external field decreases, its pressure on the FM spins lessens, such that at some critical fields, the stored energy in the exchange spring becomes sufficiently large for its unwinding. This process begins at regions where the anisotropy and exchange energies are highest. At that point, the heterogeneous FM/AFM exchange spring begins to retrieve and leads to nucleation and growth of the domains in the FM layer until the ground state is reached. It should be noted that the unwinding of the exchange spring occurs at regions where

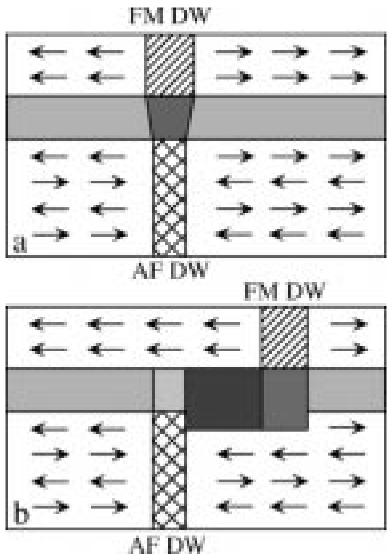

Fig. 5. Schematic representations of domain structure of (a) in the ground state of the FM/AFM bilayer, containing a hybrid FM/AFM domain wall with a line singularity connecting the FM and the AFM domains (b) during reversal of the FM, showing the formation of the exchange spring that connects, via line singularities), the moving FM domain wall and the stationary AFM domain wall. The interface region is shown in light gray.

anisotropy and energies are higher as opposed to lower energies during exchange spring nucleation. Thus, the unwinding of the exchange spring is not winding in reverse. Instead, unwinding and winding occur at different locations. This is the basis for the asymmetrical reversal of exchange-coupled systems, such as the observation of the asymmetry in the domain growth.

Finally, we discuss the origin of the influence of field direction on DW orientation revealed in this work. It is known that the DW can be entirely of one of two charalities, or a mixture of both chiralities, separated by Bloch line singularities, which separate two regions in the DW where the spins are twisted clockwise and counterclockwise [15], [20], [23]. The chirality of the FM DW determines the detailed spin structure of the line spin singularity inside the interface region. As indicated in Fig. 5(b), the moving FM DW causes an exchange spring penetrating into the AFM, whose spins are twisted according to the chirality of the FM DW. From this point on, the mobility and orientation of the FM DW is controlled by the spin singularity in the exchange spring. During reversal, the decreasing magnetic field, or magnetic field of opposite sign, lead to different spin twisting in the exchange spring in locations as well as orientation.

In summary, we have described a number of experimental results that indicate conclusively that the AFM spin structure in exchange-coupled Fe/AFM multilayers is not static. Furthermore, we have observed hybrid DWs consisting of both FM and AFM sections in the ground state of an ac demagnetized FM/AFM bilayer cooled in a zero field. Under a magnetic field, the FM DW moves, while the AFM DW remains stationary. In the process, an exchange spring develops that connects the moving ferromagnetic DW and the stationary antiferromagnetic DW. The shifted hysteresis loop (the signature of exchange bias) involves winding and unwinding of the exchange spring during the backward and forward reversals at different locations depending on the chirality of the FM DW.

ACKNOWLEDGMENT

The authors thank N. J. Gökemeijer for the samples.

REFERENCES

[1] B. Dieny, V. S. S. Speriosu, S. S. P. Parkin, B. A. Gurney, D. R. Wilhoit, and D. Mauri, “Giant magnetoresistive in soft ferromagnetic multilayers,” *Phys. Rev. B*, vol. 43, p. 1297, 1991.
[2] J. Nogues and I. K. Schuller, “Exchange bias,” *J. Magn. Magn. Mater.*, vol. 192, p. 203, 1999.
[3] A. E. Berkowitz and K. Takano, “Exchange anisotropy: A review,” *J. Magn. Magn. Mater.*, vol. 200, p. 552, 1999.
[4] R. L. Stamps, “Mechanisms for exchange bias,” *J. Phys. D: Appl. Phys.*, vol. 33, p. R247, 2000.
[5] W. H. Meiklejohn and C. P. Bean, “New magnetic anisotropy,” *Phys. Rev.*, vol. 102, p. 1413, 1956.
[6] T. Ambrose and C. L. Chien, “Dependence of exchange coupling on antiferromagnetic layer thickness in NiFe/CoO bilayers,” *J. Appl. Phys.*, vol. 83, p. 6822, 1998.
[7] V. I. Nikitenko, V. S. Gornakov, A. J. Shapiro, R. D. Shull, K. Liu, S. M. Zhou, and C. L. Chien, “Asymmetry in elementary events of magnetization reversal in a ferromagnetic/antiferromagnetic bilayer,” *Phys. Rev. Lett.*, vol. 84, p. 765, 2000.
[8] M. R. Frtzsimmons, P. Yashar, C. Leighton, I. K. Schuller, J. Nogus, and C. F. Majkrzak, “Asymmetric magnetization reversal in exchange-biased hysteresis loops,” *Phys. Rev Lett.*, vol. 84, p. 3986, 2000.
[9] N. J. Gökemeijer and C. L. Chien, “Memory effects of exchange coupling in CoO/Ni81Fe19 bilayers,” *J. Appl. Phys.*, vol. 85, p. 5516, 1999.
[10] N. J. Gökemeijer, J. W. Cai, and C. L. Chien, “Memory effects of exchange coupling in ferromagnet/antiferromagnet bilayers,” *Phys. Rev. B*, vol. 60, p. 3033, 1999.
[11] D. Mauri, H. C. Siegmann, P. S. Bagus, and E. Kay, “Simple model for thin ferromagnetic films exchange coupled to an antiferromagnetic substrate,” *J. Appl. Phys.*, vol. 62, p. 3047, 1987.
[12] N. C. Koon, “Calculations of exchange bias in thin films with ferromagnetic/antiferromagnetic interfaces,” *Phys. Rev. Lett.*, vol. 78, p. 4865, 1997.
[13] T. C. Schulthess and W. H. Butler, “Consequences of spin-flop coupling in exchange biased films,” *Phys. Rev. Lett.*, vol. 81, p. 4516, 1998.
[14] M. D. Stiles and R. D. McMichael, “Model for exchange bias in polycrystalline ferromagnet-antiferromagnet bilayers,” *Phys. Rev. B*, vol. 59, p. 3722, 1999.
[15] A. P. Malozemoff, “Random-field model of exchange anisotropy at rough ferromagnetic-antiferromagnetic interfaces,” *Phys. Rev. B*, vol. 35, p. 3679, 1987.
[16] F. Y. Yang and C. L. Chien, “Spiraling spin structure in an exchange-coupled antiferromagnetic layer,” *Phys. Rev. Lett.*, vol. 85, p. 2597, 2000.
[17] H. Ohldag, A. Scholl, F. Nolting, A. Anders, F. U. Hillebrecht, and J. Sthr, “Spin reorientation at the antiferromagnetic NiO(001) surface in response to an adjacent ferromagnet,” *Phys. Rev. Lett.*, vol. 86, p. 2878, 2001.
[18] V. I. Nikitenko, V. S. Gornakov, L. M. Dedukh, Yu. P. Kabanov, A. F. Khapikov, A. J. Shapiro, R. D. Shull, A. Chaiken, and R. P. Michel, “Asymmetry of domain nucleation and enhanced coercivity in exchange-biased epitaxial NiO/NiFe bilayers,” *Phys. Rev. B*, vol. 57, p. R8111, 1998.
[19] C. Leighton, J. Nogués, B. J. Jönsson-Åkerman, and I. K. Schuller, “Coercivity Enhancement in Exchange Biased Systems Driven by Interfacial Magnetic Frustration,” *Phys. Rev. Lett.*, vol. 84, p. 3466, 2000.
[20] A. P. Malozemoff and J. C. Slonczewski, *Magnetic Domain Walls and Bubble Materials*. New York: Academic, 1979.
[21] M. Kiwi, “Exchange bias theory,” *J. Mag. Mag. Mater.*, vol. 234, p. 584, 2001.
[22] W. H. Meiklejohn and C. P. Bean, “New magnetic anisotropy,” *Phys. Rev.*, vol. 105, p. 904, 1957.
[23] A. P. Malozemoff, “Mechanisms of exchange anisotropy,” *J. Appl. Phys.*, vol. 63, p. 3874, 1988.